Indian J. Met. Geophys. (1971), 22,23-34

551.46 : 551.553.21(267)

Oceanography of the Arabian Sea during the southwest monsoon season Part II : Stratification and circulation

J. S. SASTRY and R. S. D'SOUZA

Health Physics Division,
Bhabha Atomic Research Centre, Bombay

(Received 1 April 1970)

ABSTRACT. The distribution of mass in the Arabian Sea during the southwest monsoon season, 1963 is presented through several vertical sections and spatial distribution charts of the thermosteric anomaly. The circulation patterns in the upper 200 m are derived. The basic feature of circulation is found to be the formation of several cyclonic and anti-cyclonic cells. Upwelling off the southwest coast of India has been explained on a more rational basis than has been assumed hitherto. It is now attributed partly due to the divergence in the current field and partly due to the cyclonic motion around Laccadive and Maldive Islands.

1. Introduction

Sastry and D'Souza (1970) have earlier presented a study on the temperature distribution in the Arabian Sea during the southwest monsoon season, 1963. The authors now present the distribution of mass and the geostrophic flow patterns in the region utilising the same *Atlantis* data. The distribution of mass in the oceans has been widely studied by presenting sections and charts showing the distribution of the thermosteric anomaly (δ_T) or its related parameter σ_T. A knowledge of the distribution of either of these properties δ_T or σ_T is useful to assess the degree of stratification in the water column.

Earlier studies on the distribution of δ_T or σ_T in the Arabian Sea are mostly confined to the coastal regions. Here, the distribution of mass in the Arabian Sea is presented in greater detail by constructing several vertical sections and charts showing the distributions of δ_T. Further, the near surface flow patterns are derived on the basis of charts showing the dynamic topography of the sea surface and some subsurface levels.

2. Data and method of analysis

A brief summary of station data together with the methods of constructing various vertical sections and charts was given in Part I (Sastry and D'Souza 1970). For convenience, the station location map, Fig. 1 (of Part I) is reproduced here.

The notion of a geostrophic balance appears to be well established for oceanic regions. The usual method of dynamic computations, the geostrophic equation being the basis, has been adopted here to derive the flow patterns at surface and subsurface levels. However, one should be careful in applying this equation for several reasons.

One of the important components in the geostrophic equation becomes zero at the equator. Thus, the use of this equation to compute currents in the regions close to the equator is not much favoured till recently. However, studies by Knauss (1963) and others show that this equation holds good to within one-half degree on either side of the equator.

The accuracy in the estimates of the current by the dynamic method depends upon the accuracy in fixing the level of no motion. Stommel (1965) points out 'the fact that this all important level of no motion or reference level, is still, to all intents and purposes, undetermined, is one of the most disconcerting features of physical oceanography'. Fomin (1964) while critically reviewing the various methods to fix the level of no motion, mentions that Defant's and Sverdrup's methods, based on the continuity of water volume, when carefully applied to each individual case, yield good results. Sundara Ramam and Sreerama Murthy (1968) and Varadachari *et al.* (1968) consider the 500 decibar surface for the level of no motion. These studies are limited in space and the observations do not extend to great depths. Zaklinskii, (1964) on the other hand, considers a sloping surface and for the region of our interest, the level of no motion has depths varying from about 400 to 475 m. Swallow and Bruce (1966) compare the volume transports in the upper 200 m in the Somali Basin derived by direct current measurements and by geostrophic current estimates assuming an arbitrary reference level at 1000 m. They find good agreement between the two estimates and the discrepancies were attributed partly due to non-geostrophic flow and partly due to the motion at 1000 m.

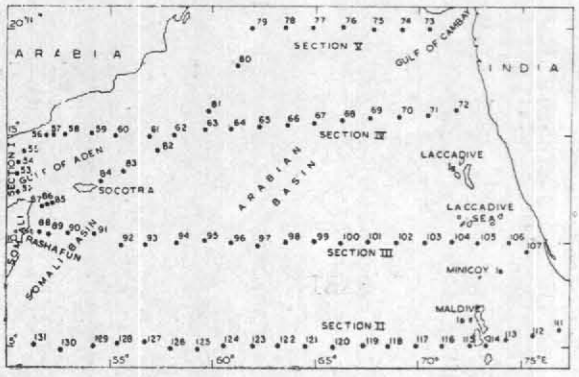

Fig. 1. Station location map

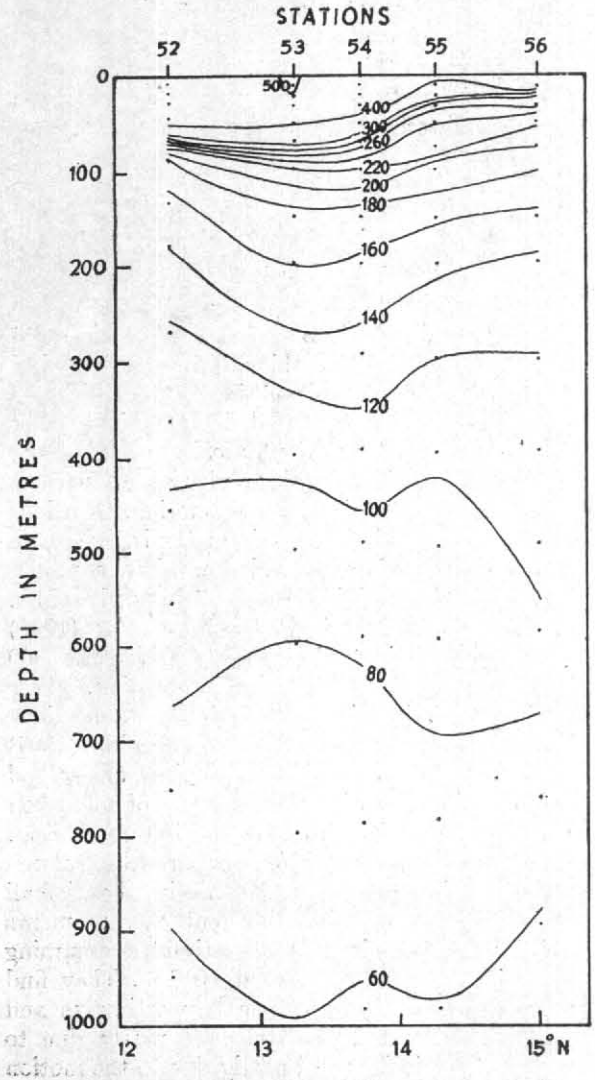

Fig. 2. Thermosteric anomaly (cl/T) along [approximately 50°E (Section I)

Application of Defant's (1941) technique to study the topography of the 'zero level' in the Arabian Sea has not yielded sufficiently good results to accept them with any reasonable degree of certainty. The selection of the reference level at a sufficiently great depth has less effect on the surface water velocities than on the deep water velocities. While an improper choice could result in wrong estimates for mass transport, the flow patterns in the upper layers are not very much altered. Keeping these aspects in view, we have arbitrarily chosen the 1500 decibar surface as the level of no motion. As will be seen in later reports, the flow patterns presented here are consistent with the distributions of other variables. After the reference level was chosen, the computations are extended into shallow regions using the method of Helland-Hansen (*see* Sverdrup, Johnson and Fleming 1942 and also Fomin 1964).

3. Distribution of δ_T

In this section, the distribution of mass is shown by presenting the distribution of δ_T along five sections (one across the Gulf of Aden and the others along 5°, 10°, 15° and 20°N). Also included are charts showing the spatial distribution of δ_T at 0, 100 and 200 m.

3.1. *Vertical sections*

Fig. 2 shows the distribution of thermosteric anomaly along Section 1, across the Gulf of Aden. At surface, the thermosteric anomaly varies from over 500 cl/T (Station 53) to 415 cl/T (Station 55). Below the surface layer*, a layer of mass discontinuity develops in the region of the thermocline as is evident by the close spacing of the isanosteres (lines of equal δ_T following Montgomery and Wooster 1954). Though the salinity distribution slightly modifies the distribution of δ_T the isanosteres, to a large extent, follow the pattern of the isotherms, since the temperature decreases rapidly with depth in the thermocline. This correspondence between the isanosteres and the isotherms can be seen upto about 200 m along this section.

It has been pointed out in Part I, that temperature inversions occur below the thermocline along this section. However, the distribution of δ_T suggests stable stratification in the entire water column indicating that the salinity distribution plays a compensating role to bring stable stratification (*see* Sastry and D'Souza 1970 a). The

*Since the surface layer and the thermocline are defined on the basis of temperature distribution alone in Part I (Sastry and D'Souza 1970) and since δ_T is a function of both temperature and salinity, only qualitative comparison can be made.

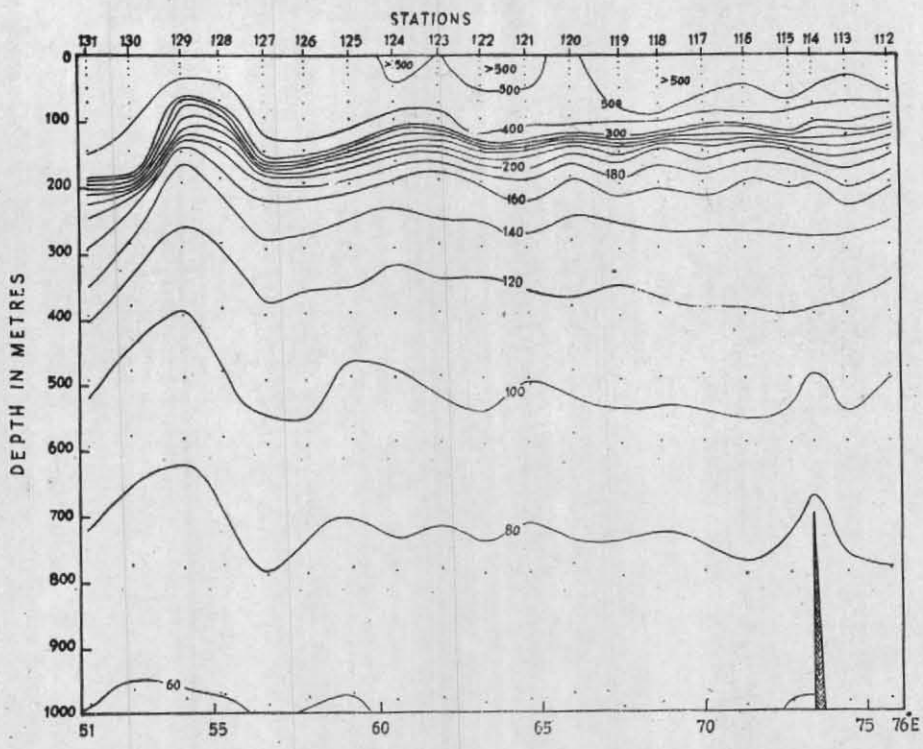

Fig. 3. Thermosteric anomaly (cl/T) along approximately 5°N (Section II)

configuration of the isanosteres (120, 100, 80 and 60 cl/T) suggests the complex nature of the field of motion as will be seen later. Fig. 2 further suggests that the flow is considerable at 1000 m.

Along 5°N, the thermosteric anomaly (Fig. 3), at surface in general, shows a west-east increase, similar to that of temperature (Sastry and D'Souza 1970). In the eastern portions along this section the values of δ_T exceed 500 cl/T with a maximum value of 577 cl/T at station 115. Off the African coast, the surface water is relatively denser and the values of δ_T are well below 500 cl/T with a minimum value of 430 cl/T at station 129. Below the surface layer, the mass discontinuity layer is strongly developed along this section. At station 129, the discontinuity layer rises close to the surface, the isanosteres forming a dome like structure with depressions on either side, an indication of a strong anti-clockwise circulation in this region. The mass distribution further suggests that the water movements are considerable even at 1000 m, especially in the Somali Basin. Below about 1600m, the thermosteric anomaly remains rather uniform with values less than 40 cl/T.

The distribution of thermosteric anomaly along Section III (Fig. 4) shows that at surface it varies from less than 400 cl/T near the Somali coast to close to 700 cl/T off the west coast of India. As mentioned in Part I, intense upwelling off the Somali coast during this season brings dense subsurface water to the surface which later spreads. As a result, the isanosteres appear to rise up towards the Somali coast. Thus the thermosteric anomaly gradually increases with increasing distance from the Somali coast. On the other hand, off the west coast of India, the high values of δ_T seem to result due to considerable dilution by excessive rainfall and land drainage during this season. Though the surface temperatures in this region are in general, slightly lower than those further south (at 5°N), the salinity distribution (Sastry and D'Souza 1970a) shows the presence of relatively less saline water ($32{\cdot}81\,^{\circ}/_{00}$ at station 106).

The isanosteres in the mass discontinuity layer in the eastern Arabian Sea are slightly inclined upwards toward the Indian coast. In the western Arabian Sea, they appear to come out off the sea surface and sink to greater depths off the Somali coast. A dome like structure of the isanosteres in the discontinuity layer is observed at stations 92 and 93 with depressions on either side centred around stations 91 and 95 respectively. Comparing this with the similar features at 5°N this is not so strongly developed.

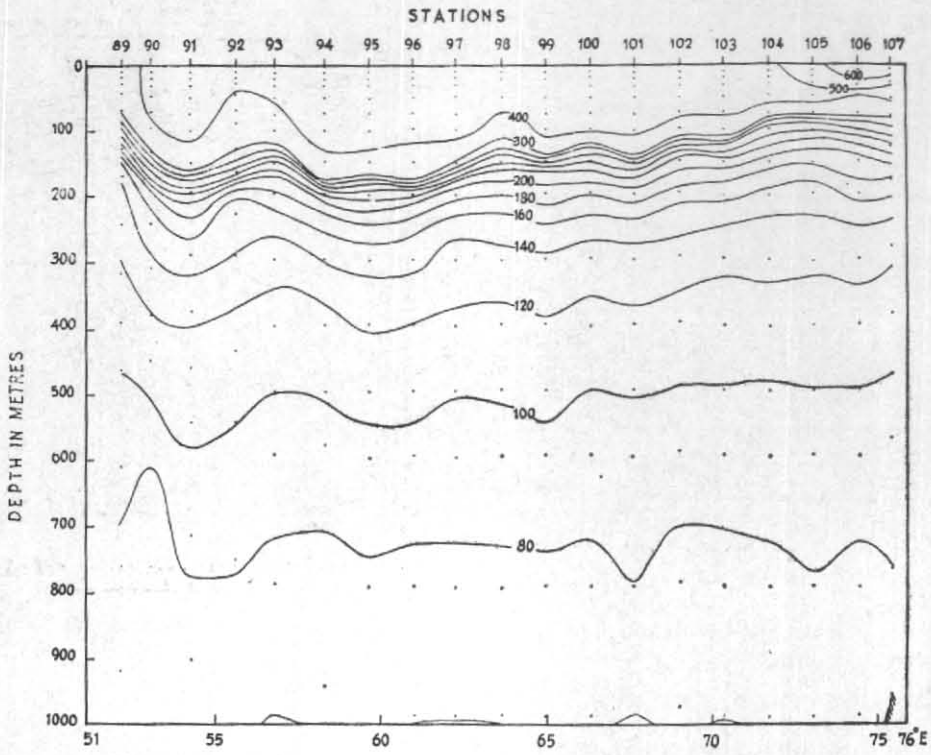

Fig. 4. Thermosteric anomaly (cl/T) along approximately 10°N (Section III)

In the intermediate layers, below 500 m, the isanosteres tend to slope downwards towards the Indian coast. Otherwise, they remain nearly horizontal, though the wavy structure is quite evident.

The thermosteric anomaly decreases to fairly uniform values (<40 cl/T) below 1600 m.

Fig. 5 shows the distribution of δ_T in Section IV along 15°N. The thermosteric anomaly at surface along this section does not show any conspicuous west-east increase as was observed along the two southern sections presented earlier. In the eastern regions along this section, δ_T is generally greater than 400 cl/T, while in the western parts it is less than 400 cl/T except in isolated regions. At station 62, consequent to the southward spreading of the dense sub-surface upwell water off the Arabian coast, the thermosteric anomaly is lowest (358 cl/T) along this section.

From the central regions of this section, the isanosteres in the mass discontinuity layer tend to rise upward both towards the Indian and African coasts. The upward rise of the isanosteres to the west associated with a wavy structure is more pronounced.

In the intermediate layers, the isanosteres tend to be horizontal, though the wavy character is quite evident.

The distribution of δ_T along 20°N (Fig. 6) shows that its variation at the surface is small varying from 395 cl/T at station 78 to 438 cl/T at station 73. The isanosteres in the mass discontinuity layer rise upward to the east.

A comparison of the distributions of δ_T along the four zonal sections (Figs. 3 through 6) suggests that the mass discontinuity layer increases in its thickness with increasing latitude. Thus, the water in the mass discontinuity layer is more strongly stratified at 5°N than further north.

Comparing these distributions with those of temperature (Sastry and D'Souza 1970) along corresponding sections, one would find a close similarity between the isanosteres and the isotherms, except in the regions where the salinity distribution affects the structure of the isanosteres to bring about stable stratification in the water column.

3.2. *Spatial distributions*

Figs. 7, 8 and 9 show the spatial distribution of δ_T at 0, 100 and 200 m respectively.

Fig. 7 shows a wide variation in δ_T at surface. It varies from about 240 cl/T ($\sigma_T = 25{\cdot}60$) to close to 700 cl/T ($\sigma_T = 20{\cdot}78$). High values are observed in the southeast Arabian Sea in contrast to low values that occur off the Somali coast. This non-homogeneous distribution of δ_T is partly due to the large spatial variations in surface temperature exceeding 11°C (Sastry and D'Souza 1970) and partly due to the surface salinity variations (Sastry and D'Souza 1970a). In the region of the cold water core extending north-northeast from station 88 (which results because of intense upwelling as mentioned in Part I) the thermosteric anomaly is lowest. With the spread of this cold upwell water over the surface further east and south, the distribution of δ_T in this region, to a large extent, resembles the temperature distribution. On the other hand, in the southeast Arabian Sea especially in the region between the west coast of India on the east and a line joining the Laccadive and Maldive Islands to the west, the surface salinity is low ($<33{\cdot}0$ o/$_{00}$ at station 106) and consequently the thermosteric anomaly has very high values. In the southern portions of the eastern Arabian Sea where the surface temperature exceeds 28·5°C the presence of relatively less saline equatorial water gives rise to moderately high values for δ_T in some isolated regions. Across the Gulf of Aden to the east of Section 1, the thermosteric anomaly decreases rapidly to a minimum to coincide with the cold water core mentioned earlier.

The distribution of thermosteric anomaly at 100 m (Fig. 8) shows that it varies from less than 180 cl/T ($\sigma_T = 26{\cdot}23$) to more than 440 cl/T ($\sigma_T = 23{\cdot}50$). The distribution is basically similar to that of temperature (Fig. 9 of Part I). Tongues of light water (> 400 cl/T) show up between 5° and 10°N interspersed by relatively dense water zones. Off Cochin, a pocket of dense water (< 260 cl/T) is centred around station 105. Off the west coast of India, the isanosteres are oriented parallel to the coast with the thermosteric anomaly increasing gradually to a maximum (> 400 cl/T) to merge with the core of light water extending northwards from stations 120 to 122. Further west, the thermosteric anomaly decreases to a minimum (< 360 cl/T) and later increases to a maximum shown by the 420 cl/T isanostere around stations 126 and 95. A tongue of dense water extends northward from stations 128 and 129 and separates the above zone from another narrow band of light water, the axis of which is located along stations 130 and 91. Further west, towards the coast of Somali, the thermosteric anomaly decreases rapidly to 180 cl/T at station 88. Between 5° and 8°N and along 50°E, the isanosteres run

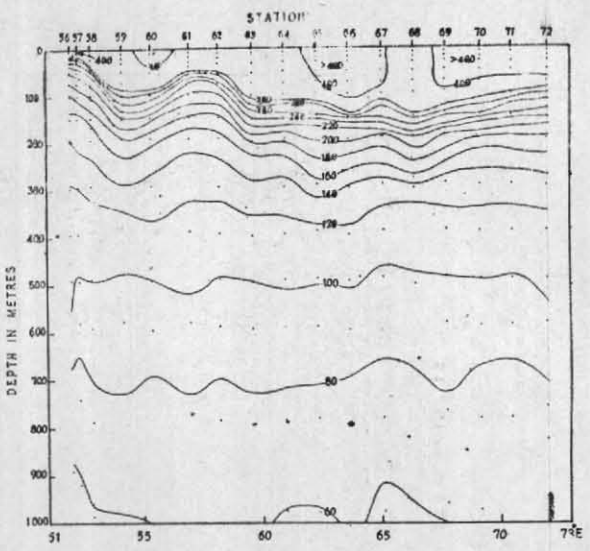

Fig. 5. Thermosteric anomaly (cl/T) along approximately 15°N (Section IV)

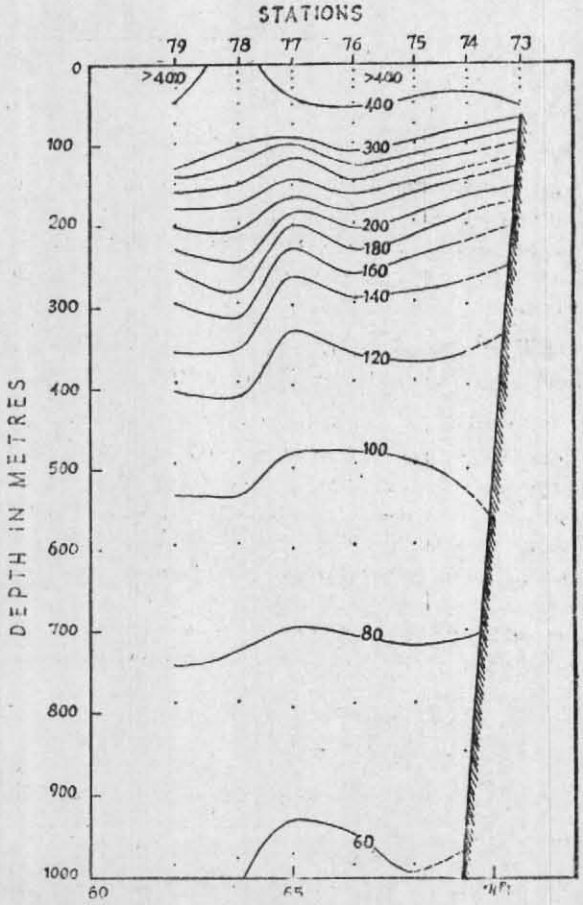

Fig. 6. Thermosteric anomaly (cl/T) along approximately 20°N (Section V)

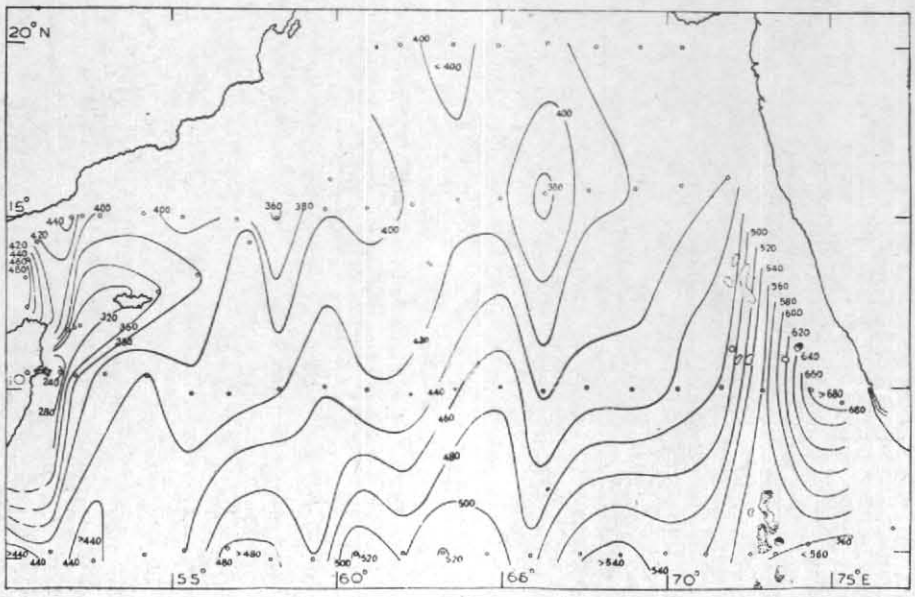

Fig. 7. Thermosteric anomaly (cl/T) at surface

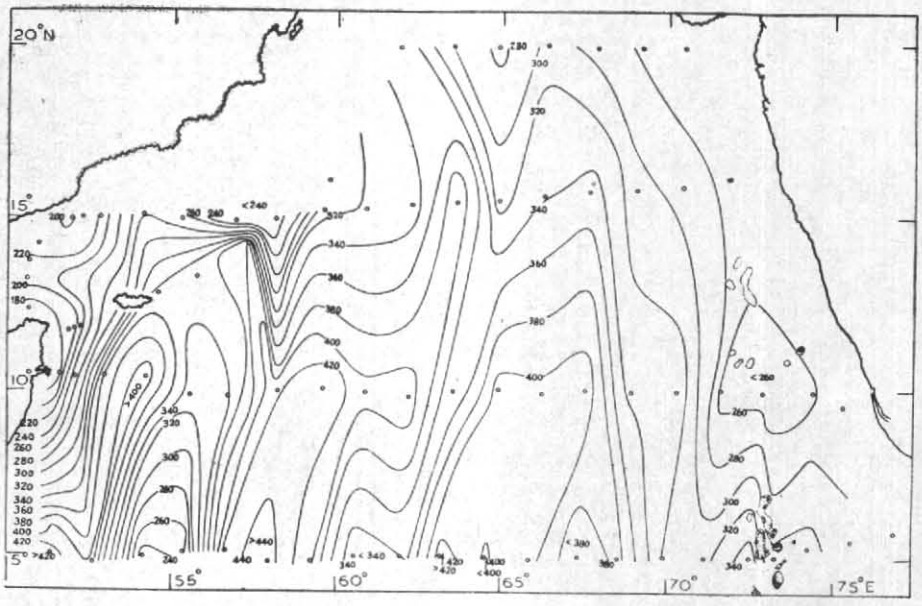

Fig. 8. Thermosteric anomaly (cl/T) at 100 m

west-east and at about 52°E, they turn abruptly to north. Across the Gulf of Aden, δ_T ranges from 178 to 215 cl/T. Centred around stations 61 and 62, a tongue of dense water extends south.

Thus, the complexity in the distribution of δ_T associated with strong lateral gradients suggest an equally complex circulation pattern on this surface. This irregularity is due to the location of this surface in the homogeneous surface layer at some places and in the mass discontinuity layer at other places (*see* also Sastry and D'Souza 1970).

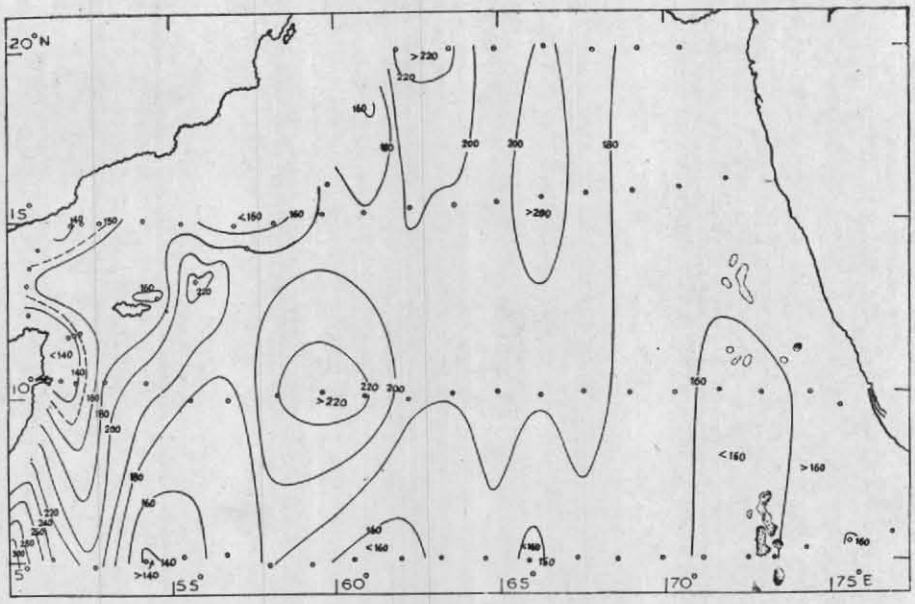

Fig. 9. Thermosteric anomaly (cl/T) at 200 m

Fig. 9 shows the distribution of thermosteric anomaly at 200 m. In contrast to the complex distribution of δ_T at 100 m, its distribution over this surface is relatively simple. The values of δ_T range from over 130 cl/T (σ_T = 26·75) to about 230 cl/T (σ_T = 25·70). In the extreme south-western regions, however, it exceeds 330 cl/T (at station 132, not shown in figure). The temperature and salinity distribution at 200 m in the eastern Arabian Sea are such that they increase to north and northwest. Thus, the effect of increase in temperature on δ_T is largely compensated by the increase in salinity and the close correspondence between the isanosteres and the isotherms which was apparent at 100 m is not observed on this surface in this region. The spatial gradients of δ_T over this surface in the eastern regions are small. However, in the western Arabian Sea, west of 62°E, there is considerable similarity between the distributions of the thermosteric anomaly and of temperature. Thus the warm water pockets, one centred around station 95 and the other enveloping stations 130 and 91 can be identified as light water pockets in the δ_T distribution.

The thermosteric anomaly at 500 m (not shown here) varies within a narrow limit from about 93 cl/T (σ_T = 27·14) to about 107 cl/T (σ_T=27·00). The isotherms and the isohalines over this surface are oriented in a west-east direction and both the parameters increase to the north. However, the distribution of δ_T is irregular and the isanosteres do not show any corresponding orientation either with the isotherms or with the isohalines. Even though the variation in δ_T over this surface is small, one can identify zones of lighter water (surrounding stations 91 and 95) and relatively denser water (at station 129 and in the regions west of Laccadive Islands). The gradients of δ_T are generally weak.

The distribution of δ_T at 1000 m shows that it varies from 56 cl/T (σ_T = 27·54) to 65 cl/T(σ_T = 27·44). At 1500 m the variation in δ_T is from 38·5 cl/T (σ_T = 27·72) to 46 cl/T (σ_T = 27·64). At both these levels the gradients are weak.

In the intermediate layers (500, 1000 and 1500 m) there appears a considerable small scale (horizontal) structure. The station spacing is in hundreds of kilometers and as such the finer details in the distributions of δ_T at these levels are probably lost.

4. Circulation

So far, our main concern was to analyse the mass distribution with a view to study the stratification on the water mass in the Arabian Sea. In this section, we present the geostrophic currents across the Gulf of Aden and the near surface circulation patterns in the region by presenting the dynamic topography charts for 0, 100 and 200 decibar levels.

Before discussing the flow patterns, it is well to remember that these are based on observations collected over a period of two months and that a

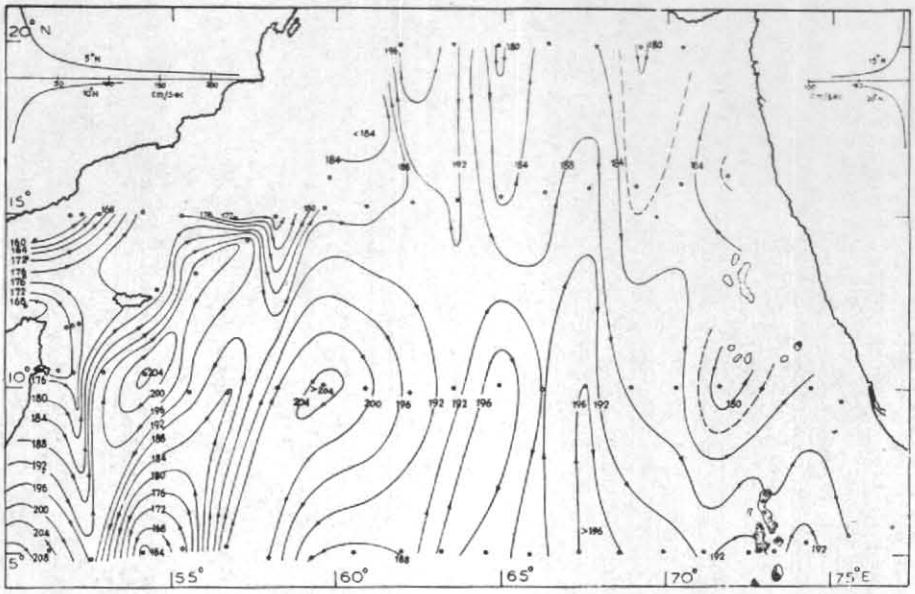

Fig. 10. Dynamic topography of the sea surface relative to 1500 decibars (dy. cm)

steady state is assumed during the interval. However, the studies in the Somali Basin by Warren, Stommel and Swallow (1966) and Swallow and Bruce (1966) indicate that the currents are highly variable in space and time and one should be cautious in interpreting and drawing conclusions from these patterns. Hence no attempt has been made here to estimate the volume transports.

4.1. *Near surface circulation*

We now present the dynamic topography charts for the 0, 100 and 200 decibar levels (Figs. 10, 11 and 12 respectively) relative to the 1500 decibar surface to present the near surface circulation. In these figures, the isopleths are in dynamic centimeters. The arrows indicate the direction of flow and the speed can be obtained from the inset diagrams.

The spatial variation of the geopotential anomaly is maximum (about 55 dy. cm) at surface and this variation decreases with depth. At 200 m the spatial variation is 21 dy. cm while at 500 m (not shown here) it is less than 10 dy. cm. These features suggest that the flow is mostly confined to upper layers. It further suggests that the surface circulation patterns would not have altered much even if the shallower 500 decibar surface was chosen for the reference level.

In Fig. 10, the isolines are drawn at intervals of 4 dy. cm while in Figs. 11 and 12, the interval is 2 dy. cm except as shown otherwise.

The basic feature of near surface circulation, west of 62°E, is the formation of several clockwise and anti-clockwise cells or 'whirls' which appear to extend to depths of 200 m and deeper. North of 5°N, off the African coast, the Somali current turns east and splits into two branches one turning north and the other south. North of 10°N the northern branch splits again into two streams. One branch follows the coast and turns west into the Gulf of Aden (*see* Fig. 13) while the other turns northeast in the region south of Socotra and later flows on the eastern side of Socotra and finally merges with the clock-wise cell centred around station 91. Thus, a part of the water originating in the Somali current returns south as far as 5°N and appears to reinforce the southern branch of the Somali current. At 5°N and 55°—56°E (between stations 127 and 128) the north component of the geostrophic current (at surface) exceeds 150 cm/sec. This, as it moves north, splits into two streams. One branch turns west and then to south strengthening the southern branch of the Somali current mentioned above. Thus, between stations, 129 and 130, the southerly flow exceeds 160 cm/sec at surface. The second branch (originating at stations 127 and 128) flows further north and finally merges in another clockwise cell centred around station 95 and a part of this water probably returns to 5°N between stations 125 and 126. Separating these two clockwise whirls (around stations 91 and 95) in the north, a cyclonic circulation pattern is observed southward of station 62. In the northern regions of the

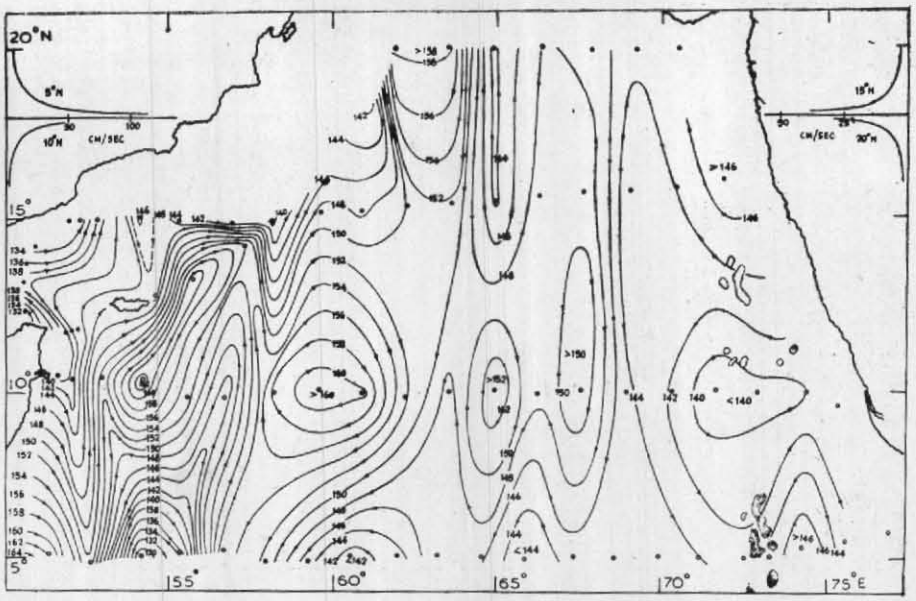

Fig. 11. Dynamic topography of the 100 decibar surface relative to 1500 decibar (dy. cm)

Gulf of Aden, the flow is to east and eastnortheast. In the southeast Arabian Sea, the surface circulation is cyclonic. Off Ratnagiri (around station 72), an anti-cyclonic circulation is observed.

In the northwestern Arabian Sea, between stations 77 and 78, the flow is directed south and south of 15°N, this flow branches into two, one merging with the cyclonic circulation in the southeastern Arabian Sea and the other turning northwest. Just west of the cyclonic circulation pattern in the southeast Arabian Sea, two clock-wise cells are found.

The circulation patterns at 100 and 200 m (Figs. 11 and 12 respectively) are basically similar to those at surface (Fig. 10).

Thus, as a whole, the near surface circulation is quite complex and several cyclonic and anti-cyclonic cells with varying intensity characterise the entire region. This necessitates considerable vertical movements (both sinking and upwelling) in the entire region as redistribution of mass takes place.

Swallow and Bruce (1966) quoting Findlay mention about the existence of a great (clock-wise) whirl in the Somali Basin. Their studies during the southwest monsoon of 1964 in the Somali Basin further revealed yet another clock-wise whirl south of Socotra. Our studies in this region show basically similar circulation patterns suggesting that the circulation patterns derived here are more or less characteristic of the southwest monsoon season.

Rama Sastry (1968) while discussing the sub-surface salinity distribution below the mass discontinuity layer in the eastern Arabian Sea, especially off the west coast of India, intuitively infers that the flow off the coast should be directed to north and northwest along the coast and to south farther away from the coast. He further reasons that the flow should be cyclonic around the Laccadive Islands. The sub-surface circulation patterns presented in Figs. 11 and 12 confirm his reasoning.

The dynamic topography chart at 500 decibars (not given here) shows a relatively small variation (<10 dy. cm) indicating a rather sluggish character of flow at this level. It has been pointed out earlier that the station spacing is such that the finer details in the distributions of δ_T could not be brought about in the intermediate layers. In view of these aspects and keeping in mind the inherent limitations in using the geostrophic equation, it is felt that a proper assessment of the flow at these levels is not possible. An attempt will, however, be made later to present the flow at these levels by studying the property distributions on surfaces of constant thermosteric anomaly.

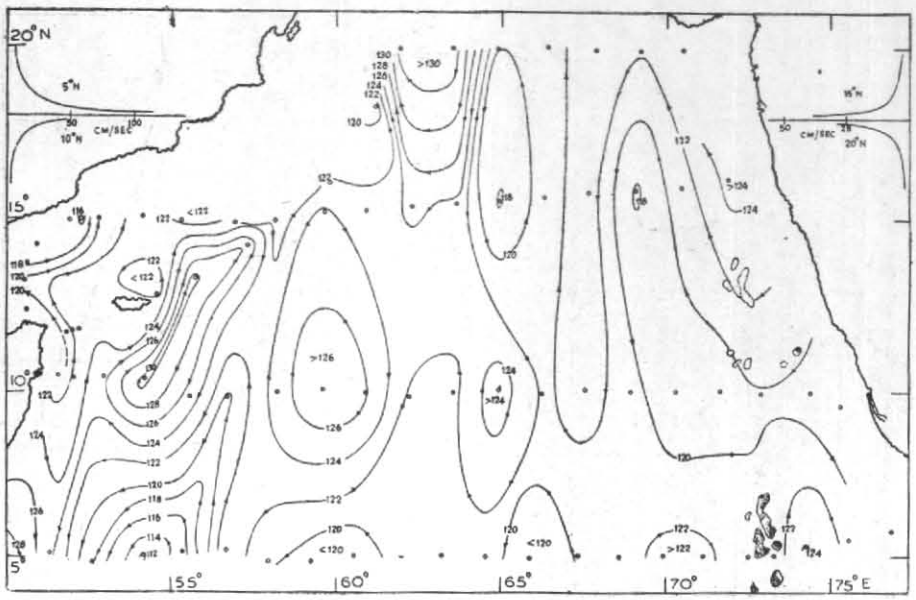

Fig. 12. Dynamic topography of the 200 decibar surface relative to 1500 decibar (dy. cm)

4.2. *Geostrophic currents across the Gulf of Aden*

The thermal structure, the T-S curves (Fig. 2 and Fig. 7 respectively of Sastry and D'Souza 1970) and the distribution of salinity (Sastry and D'Souza 1970a) and of δ_T (Fig. 2) across the Gulf of Aden are all complex and it would be of interest to analyse the field of motion in this region. Fig. 13 shows the geostrophic currents across the Gulf of Aden along Section 1.

In the southern Gulf, the surface flow into the Gulf exceeds 30 cm/sec between stations 52 and 53. This inflow is more or less maintained in the entire vertical column, though the speed decreases rapidly with depth and is almost negligible below 1300 m. North of station 53, the direction of surface flow is reversed and the outflow from the Gulf exceeds 50 cm/sec in the core situated between stations 54 and 55. While the current speed decreases with depth rapidly, the axis of the core shifts south with depth and is located between stations 53 and 54 at depths between 500 and 1500 m. North of this axis, in a layer extending from about 250 to 1500 m an inflow into the Gulf with a maximum speed of 4 cm/sec is observed. In the intermediate layers, the flow again reverses in the northern regions of the Gulf. Thus, in the intermediate layer, the direction of flow alternates across the Gulf of Aden. Fig. 13 also indicates that there is considerable movement of water below 1500 m. The current shear, lateral as well as vertical appears to be considerable and mixing can be quite effective. The complex character of the T-S curves across the Gulf of Aden seems to be the result of mixing.

4·3. *Upwelling off the southwest coast of India*

Several workers reported upwelling off the southwest coast of India during the southwest monsoon season. However, the mechanisms that bring about upwelling in this region have been variously described. Banse (1959, 1968), for example, stresses the importance of wind induced divergence. He reasons that the dense sub-surface water rises along the coast associated with the southeasterly coastal current which sets in during this season. He further feels that the coastal orientation and the wind distribution aid the process of upwelling. Darbyshire (1967), on the other hand, considers the advective processes to be important and suggests that the retreat of the equatorial surface water to the south results in upwelling.

However, a closer examination of Figs. 10, 11 and 12 reveals that neither of these mechanisms could be of prime importance. Fig. 10 shows that the surface flow, south of about 10°N is southeasterly as visualised by Banse. But, north of 10°N, as mentioned earlier, the flow tends to be either northerly or northwesterly along the coast. The southeasterly current is indicated only far off shore. Even at sub-surface levels (Figs. 11 and 12) the flow patterns are basically the same. Thus, the field of motion at surface and sub-surface levels shows considerable divergence off the southwest coast of India on the east

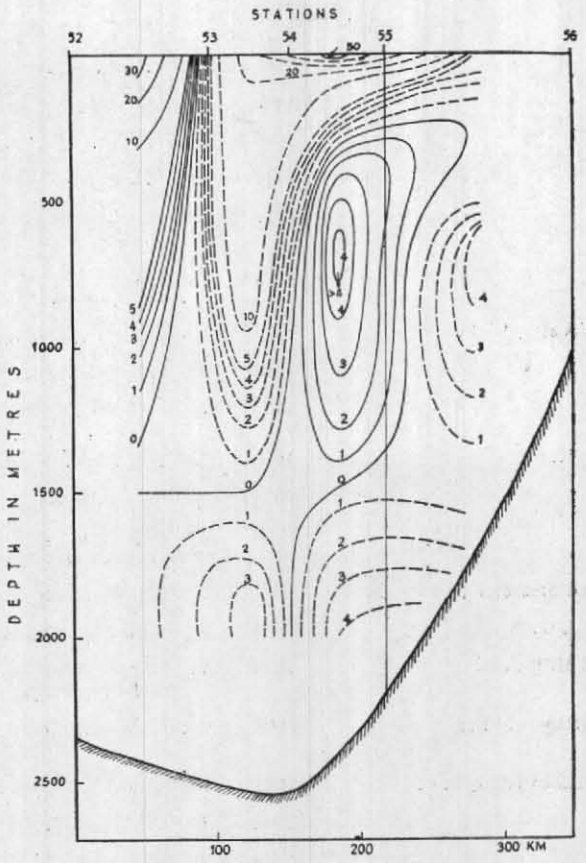

Fig. 13. Geostrophic currents (cm/sec) along Section I

--- East (into the Arabian Sea)

—— West (into the Gulf of Aden)

and the cyclonic cell centred around station 104 on the west. At 100 m, one can see this pattern well defined and more pronounced. This current divergence, for reasons of continuity in the mass distribution requires vertical movement of water (in this case upwelling). Thus, it is clear that upwelling off the southwest coast of India results because of divergence in the current field. This current field itself is probably a result of the modification by the complicated bottom topography in the neighbourhood of the Laccadive and Maldive islands.

The dynamic topography charts presented by Sundara Ramam and Sreerama Murthy (1968) using 'Kistna' data for June-August 1963, indicate southeasterly flow only south of 10°N, while north of 10°N, no southeasterly flow is present. Thus, Banse's reasoning may apply to the extreme southwestern coastal regions and upwelling as visualised by him could be only of a limited extent. It is not exactly clear from these data at hand the nature and extent of upwelling as suggested by Darbyshire. The retreat of the equatorial water to the south may be a secondary effect coupled with the divergence phenomenon mentioned above.

It has been pointed out earlier that vertical movements are likely associated with the cyclonic and anti-cyclonic cells. Reid (1967) while discussing the various processes of upwelling mentions that upwelling results from cyclonic motion of the wind-driven, quasi-geostrophically balanced flow. Wyrtki (1964) associates upwelling in the Costa Rica Dome with the cyclonic flow around the Dome. It is probable that upwelling of a considerable extent may occur in the region of the cyclonic circulation in the neighbourhood of the Laccadive and Maldive Islands.

Acknowledgements

We wish to thank Dr. A.K. Ganguly, Head, Health Physics Division, Bhabha Atomic Research Centre, for his interest in this work. This work is carried out under the Research Agreement No. 155/R5/CF between the International Atomic Energy Agency and the Bhabha Atomic Research Centre.

REFERENCES

Banse, K.	1959	*J. Mar. Biol. Ass. India*, **1** (1), pp. 33-49.
	1968	*Deep-Sea Res.*, **15**, pp. 45-79.
Darbyshire, M.	1967	*Ibid.*, **14**, pp. 295-320.
Defant, A.	1941	*'Meteor' 1925-1927*, 6, Pt. 2, 5.
Fomin, L. M.	1964	*The Dynamic Method in Oceanography*. Elsevier Publishing Co., Amsterdam-London-New York.
Knauss, J. A.	1963	*The Sea*, **2**, Intersci. Publ., John Wiley & Sons Inc., London, Ch. 10.
Montgomery, R. B. and Wooster, W. S.	1954	*Deep-Sea Res.*, **2**, pp.. 68-70
Rama Sastry, A. A.	1968	Symp. Indian Ocean, Nat. Inst. Sci. India, Delhi.
Reid, J. L.	1967	*International Dictionary of Geophysics*, Pergamon, New York, pp. 1639-1640.
Sastry, J. S. and D'Souza, R. S.	1970	*Indian J . Met. Geophys.*, **20**, 3, pp. 367-382.
	1970a	(To be published.)
Stommel, H.	1965	*The Gulf Stream* ,Univ. California Press, Berkeley, Los Angeles and Cambridge Univ. Press, London.
Sundara Ramam, K. V. and Sreerama Murthy, K. V.	1968	Symp. Indian Ocean, Nat. Inst. Sci. India, Delhi.
Swallow, J. C. and Bruce, J. G.	1966	*Deep-Sea Res.*, **13**, pp. 861-888.
Sverdrup, H. U., Johnson, M. W. and Fleming, R. H.	1942	*The Oceans*, Asia Publ. House, Bombay, Calcutta, New Delhi, Madras, London and New York.
Varadachari, V. V. R., Murthy, C. S. and Das, P. K.	1968	Symp. Indian Ocean, Nat. Inst. Sci. India, Delhi.
Warren, B. Stommel, H. and Swallow, J. C.	1966	*Deep-Sea Res.* **13**, pp. 825-860.
Wyrtki, K.	1964	*Fish. Bull.*, **63**, 2.
Zaklinskii, G. B.	1964	*Deep-Sea Res.*, **11**, 286-292 (English translation).